

PAPER REF: 6528

EQUIVALENT PLATE MODEL OF CURVILINEAR STIFFENED PANELS

Francesco Danzi^(*), Enrico Cestino¹, Giacomo Frulla¹, James M. Gibert²

¹Department of Mechanical and Aerospace Engineering (DIMEAS), Politecnico di Torino, Torino, Italy

²School of Mechanical Engineering, Purdue University, West Lafayette (IN), USA

^(*)*Email:* francesco.danzi@polito.it

ABSTRACT

This manuscript presents the derivation of a systematic set of equations for the evaluation of equivalent plate model of curvilinear stiffened panels. The homogenized properties of the stiffened panel are derived by first imposing kinematic equivalence between the stiffener's strains and the strains of the equivalent layer, and then equating the strain energy density among the stiffeners and the equivalent layer among the real and the equivalent structure. The derivation is based on the first-order transverse-shear deformation theory for anisotropic plates (Reissner-Mindlin type). The stiffeners are modelled consistently using the FSDT beam theory (Timoshenko). It has been demonstrated that, if the stiffener are curvilinear, the derivation can be extended in order to derive the apparent engineering constants of the stiffened layer. A comparative study has been performed to evaluate the number of sub-cells necessary to approach the asymptotic value of the stiffnesses. The effect of the stiffeners' geometry onto the engineering constant has been investigated. To assess the validity of the proposed method, a comparative study of the buckling loads obtained with a 2D shell model and those obtained with the equivalent plate/material model is carried out.

Keywords: anisotropic structures, curvilinear stiffened panel, homogenization theory, equivalent properties, buckling loads.

INTRODUCTION

The ongoing revolution in Computer Aided Design and manufacturing technologies has broken down the barriers and paved the way to a variety of innovative solutions such as, but not limited to, VAT (Variable Angle Tow) laminates and curvilinear stiffeners (Gürdal, 2008, Kapania, 2005). The design space for the aeroelastic tailoring is being significantly enlarged. Particularly, the local stiffening effects introduced by these innovative configurations may allow unconventional structural coupling and postpone critical aeroelastic phenomena otherwise typical of wing with High Aspect Ratio (HAR) (Kapania, 2005, Martins, 2014 and Cestino, 2014).

Homogenization theories as well as surrogate models have been widely used in calculating effective properties of reinforced shells and plates. Homogenization is particularly useful in early stages of building-block analysis for navigating the design space and identifying, at a glance, optimal preliminary configurations. The earliest works on equivalent stiffnesses of stiffened plates and shells are dated back to the beginning of last century (Huber, 1914) and Flugge, 1932 respectively. In Smith, 1946, presented an improved formulation, with respect to the one of Huber, which accounts for variations in the neutral-surface position associated with

local interactions between the skin and the stiffener. A more accurate treatment of shear stresses with respect to Huber's work was presented in Pfluger 1947. In Gomza, 1948, they derived the effective plate thickness of stiffened plate. In Benscoter, 1952 they presented an equivalent-plate theory, based on first-order difference equations, that includes transverse-shear deformations. In Dow, 1953 they provide expressions for 12 independent elastic constants of isotropic plates with integral stiffeners. The expressions for the elastic constants were obtained by identifying the fundamental repeating element of the stiffened plate and then replacing each stiffener in the repeating element with a homogeneous orthotropic plate. The resulting homogeneous plate is perfectly bonded to the skin plate. The strains in the repeating-element stiffeners are related to the corresponding plate strains and the strain energy element is determined in terms of the equivalent-plate strains. Crawford, 1955 presented a study that focused on the torsional stiffness of orthogonally stiffened plates. Between 1955 and 1957, Hoppmann and his colleagues conducted experiments to determine the bending and twisting stiffnesses of orthogonally stiffened plates. Huffington, 1956 published an analysis for determining the equivalent-plate stiffnesses for orthogonally stiffened plates without stiffener eccentricity with respect to the plate skin namely, concentric configuration.

Heki, 1971 derived the closed form expressions for the stiffnesses associated with the homogeneous isotropic stiffeners with negligible in-plane shear stiffnesses.

In Won, 1990 they presented a set of equations for homogeneous isotropic beam members with rectangular cross-sections of equal depth and negligible transverse-shear stiffnesses. The expressions given by Won, 1990 are for a pair of oblique stiffener families and include higher-order effects associated with the interaction of the plate wall with the stiffeners at the stiffener intersections. Pshenichnov, 1993 published a monograph dealing with reticulated plates and shells, with an emphasis on single-layer plate-like and shell-like lattice structures in which the stiffeners are concentric. The equivalent stiffnesses presented are based on a classical shell theory and are obtained by using tensor transformations to equate beam strains with corresponding shell strains and by equating shell stress resultants with transformed beam forces that are uniformly distributed across an equivalent shell wall. Although the analysis is based on a classical shell theory, the effects of stiffener bending in the tangent plane is included expressing the beam shearing forces that act in the tangent plane in terms of the derivatives of the corresponding beam moments. The beam bending strain is obtained in terms of the shell tangential displacements and strains by considering deformation associated with rotation about the unit vector normal to the middle surface. Although this approach captures tangential stiffener bending effects, the effects cannot be represented directly in terms of the shell strains and, as a result, do not enter into the equivalent stiffness expressions for plate-like and shell-like lattices. In Jaunky, 1995 a refined smeared-stiffener theory for grid-stiffened laminated-composite is presented. The refinement presented in their work accounts for the variation of the neutral surface caused by interactions between the skin and the stiffeners. In Chen, 1996 they presented the equivalent stiffnesses for laminated-composite flat plates and circular cylindrical shells stiffened by a grid of beams. In their study, generally laminated walls stiffened with ribs, stringers, and a pair of identical diagonal stiffeners with an arbitrary orientation angle were considered. Grid-stiffness expressions are given that include out-of-plane (transverse) and in-plane shear flexibility of the stiffeners and in-plane stiffener bending. In Slinchenko, 2001 they derived the equivalent stiffnesses for homogeneous isotropic stiffeners with negligible in-plane shear and torsional stiffnesses.

Stiffened panels with curvilinear stiffeners, have been firstly introduced by Kapania and co-workers (Kapania, 2000, Tamijiani, 2009, Mulani 2010) and considered also from other researchers (Martins, 2014, Wang, 2015).

To the authors' knowledge, none of the works published to date on curvilinear stiffeners presents a set of consistent equations that associate the homogenized properties to the stiffeners' path. In Nemeth, 2011 a set of consistent equations for equivalent plate model, limited to straight stiffeners, oriented with a prescribed angle is given. In this work, we extend the derivation to curvilinear concentric stiffeners. The orientation of the stiffeners may vary between $+45^\circ$ and -45° , according to the equation given in Wu, 2002 and Wang, 2015. Using a homogenization method, based on strain-energy density equivalence, we derive the stiffnesses of the equivalent stiffener layer. The homogenization method presented herein is a hybridization of the methods used in Nemeth, 2011 to deal with lattice reinforcements. Furthermore, we extend the derivation in order to identify the apparent engineering constants of the equivalent-stiffener layer. We demonstrate analytically that the equivalent material can be found if the stiffeners are curvilinear. We limited the derivation to one family of concentric stiffeners rather than two families; this latter configuration is known as lattice structures.

STRUCTURAL MODEL

The derivation of the structural model follows the same procedure used by Dow, 1953, and Nemeth 2011 and Cestino, 2014. The strains of the repeating-element stiffeners are related to the corresponding plate strains by imposing the kinematic equivalence. Furthermore, the plate stresses' resultants are related to the beam forces and moments. The kinematic and static equivalence are referred hereafter as direct compatibility. Following Nemeth, we neglected the variation of the stress resultant across the width of the stiffeners. We extended the derivation to account for curvilinear stiffeners.

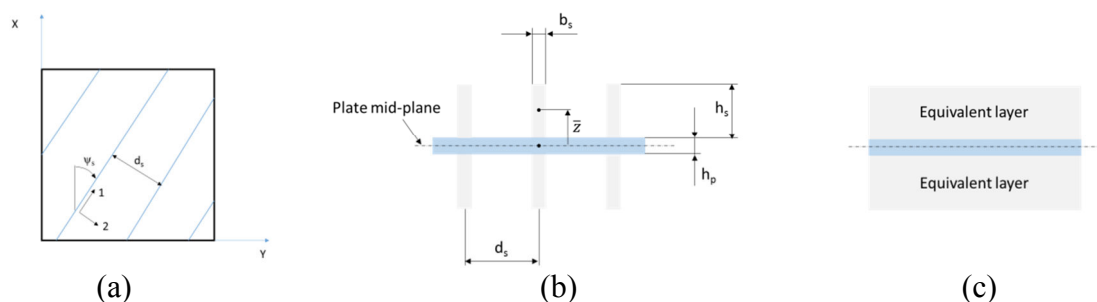


Fig. 1 - Stiffened plate top view (a), side view (b) and equivalent plate model (c)

The direct compatibility is derived for a family of rectilinear and equally spaced stiffeners (stiffener's spacing, d_s); the stiffeners are presumed being oriented with an angle ψ_s with respect to the x -axis of the plate. We assumed that the prismatic rectangular stiffeners are in the symmetric (or concentric) configuration and perfectly bonded to the isotropic skin panel. The material points of the beam are located on the local Cartesian coordinates $\langle 1, 2, 3 \rangle$, which follow the stiffeners orientation as shown in Figure 1(a). The kinematic equivalence is obtained based on the presumption that the strains at any point of the stiffener are identical to the strains at the corresponding point in the equivalent-stiffener layer. It is also presumed that the variation of strains across the width of the equivalent-stiffener layer can be neglected, i.e. the bending of the stiffener in the plane parallel to the plate mid-plane is negligible. Furthermore, the stiffener contribution to the corresponding overall plate strains is averaged; that is, to take into account that the eccentric stiffeners contribute only to half of the shear and twisting stiffnesses.

To establish the static equivalence, the stress resultants of the equivalent plate, expressed in the global coordinate system $\langle xyz \rangle$, have to be equal to the beam's forces and moments

(Timoshenko's beam). After some algebraic manipulations omitted for the sake of brevity one have¹:

$$N_x^{stiff} = \frac{EA_s}{d_s} (\varepsilon_{xx}^0 + \bar{z}k_{xx}) \quad (1a)$$

$$N_{xy}^{stiff} = \frac{k_y GA_s}{2d_s} (\gamma_{xy}^0 + \bar{z}k_{xy}) \quad (1b)$$

$$M_x^{stiff} = \frac{EA_s \bar{z}}{d_s} \varepsilon_{xx}^0 + \frac{EI_{yy}}{d_s} \bar{z}k_{xx} \quad (1c)$$

$$M_{xy}^{stiff} = \frac{k_y GA_s \bar{z}}{2d_s} \gamma_{xy}^0 + \frac{GJ_t}{2d_s} k_{xy} \quad (1d)$$

$$Q_{xz}^{stiff} = \frac{k_z GA_s}{d_s} \gamma_{xz}^0 \quad (1e)$$

The constitutive equations for the stiffeners, in terms of the strain expressed in the equivalent plate, can be written as follows:

$$\begin{Bmatrix} N_x \\ N_y \\ N_{xy} \end{Bmatrix} = \begin{bmatrix} \frac{EA_s}{d_s} & 0 & 0 \\ 0 & 0 & 0 \\ 0 & 0 & \frac{k_y GA_s}{4d_s} \end{bmatrix} \begin{Bmatrix} \varepsilon_{xx}^0 \\ \varepsilon_{yy}^0 \\ \gamma_{xy}^0 \end{Bmatrix} + \begin{bmatrix} \frac{EA_s \bar{z}}{d_s} & 0 & 0 \\ 0 & 0 & 0 \\ 0 & 0 & \frac{k_y GA_s \bar{z}}{4d_s} \end{bmatrix} \begin{Bmatrix} k_{xx} \\ k_{yy} \\ k_{xy} \end{Bmatrix} \quad (2a)$$

$$\begin{Bmatrix} M_x \\ M_y \\ M_{xy} \end{Bmatrix} = \begin{bmatrix} \frac{EA_s \bar{z}}{d_s} & 0 & 0 \\ 0 & 0 & 0 \\ 0 & 0 & \frac{k_y GA_s \bar{z}}{4d_s} \end{bmatrix} \begin{Bmatrix} \varepsilon_{xx}^0 \\ \varepsilon_{yy}^0 \\ \gamma_{xy}^0 \end{Bmatrix} + \begin{bmatrix} \frac{EI_s}{d_s} & 0 & 0 \\ 0 & 0 & 0 \\ 0 & 0 & \frac{GJ_s}{4d_s} \end{bmatrix} \begin{Bmatrix} k_{xx} \\ k_{yy} \\ k_{xy} \end{Bmatrix} \quad (2b)$$

$$\begin{Bmatrix} Q_{yz} \\ Q_{xz} \end{Bmatrix} = \begin{bmatrix} 0 & 0 \\ 0 & \frac{k_z GA_s}{4d_s} \end{bmatrix} \begin{Bmatrix} \gamma_{xz} \\ \gamma_{yz} \end{Bmatrix} \quad (2c)$$

Finally, performing the rotation to align the beam's reference system <123> to the plate reference system <xyz> one can obtain the expressions of the stiffness matrices of the usual Reissner-Mindlin plate. In the plate reference system the equivalent stiffener layer, results in a completely anisotropic material. The explicit expressions of the stiffnesses associated to the stiffener layer are reported in Eq. (3).

$$\begin{aligned} \bar{Q}_{11}^{stiff} &= \frac{E_s b_s}{d_s} \cos^2 \psi_s (\cos^2 \psi_s + \tau_y^s \sin^2 \psi_s) & ; & \quad \bar{Q}_{12}^{stiff} = \frac{E_s b_s}{d_s} \sin^2 \psi_s \cos^2 \psi_s (1 - \tau_y^s) \\ \bar{Q}_{16}^{stiff} &= \frac{E_s b_s}{d_s} \sin \psi_s \cos \psi_s \left(\cos^2 \psi_s - \frac{\tau_y^s}{2} \cos 2\psi_s \right) & ; & \quad \bar{Q}_{22}^{stiff} = \frac{E_s b_s}{d_s} \sin^2 \psi_s (\sin^2 \psi_s + \tau_y^s \cos^2 \psi_s) \\ \bar{Q}_{26}^{stiff} &= \frac{E_s b_s}{d_s} \sin \psi_s \cos \psi_s \left(\sin^2 \psi_s + \frac{\tau_y^s}{2} \cos 2\psi_s \right) & ; & \quad \bar{Q}_{66}^{stiff} = \frac{E_s b_s}{d_s} \left(\sin^2 \psi_s \cos^2 \psi_s + \frac{\tau_y^s}{4} \cos^2 2\psi_s \right) \end{aligned} \quad (3)$$

$$\begin{aligned} \bar{Q}_{44}^{stiff} &= \frac{E_s b_s \tau_z^{stiff}}{d_s} \sin^2 \psi_s \\ \bar{Q}_{45}^{stiff} &= \frac{E_s b_s \tau_z^{stiff}}{d_s} \sin \psi_s \cos \psi_s \\ \bar{Q}_{55}^{stiff} &= \frac{E_s b_s \tau_z^{stiff}}{d_s} \cos^2 \psi_s \end{aligned}$$

¹ The complete derivation for the equations in (1) is given in Nemeth, 2011

where $\tau_y^s = k_y^s \frac{G_s}{E_s}$, $\tau_z^s = k_z^s \frac{G_s}{E_s}$ are the in-plane and transverse shear-deformation parameters,

k_y^s and k_z^s are the in-plane and transverse shear correction factor, E_s is the Young's Modulus of the stiffener, b_s and d_s are the stiffeners width and spacing respectively. It should be noted that the resulting matrix \bar{Q} for the straight stiffener is singular; particularly, from the equation in (2) is worth nothing that, the rank is 2. If one aim to derive the equivalent properties of the UD material, one have:

$$E_{11} = \left(\frac{E_s b_s}{d_s} \right)_{el-12}; E_{22} = 0; \nu_{12} = 0; G_{12} = \frac{\tau_y^s}{4} \left(\frac{E_s b_s}{d_s} \right)_{el-12}; G_{13} = \tau_z^s \left(\frac{E_s b_s}{d_s} \right)_{el-12}; G_{23} = 0 \quad (4)$$

Let us consider a family of curvilinear stiffener. The local orientation of the stiffeners is presumed to vary linearly according to equation proposed by (Wu, 2002 and Wang, 2015), that is: $\psi(x) = \psi_1 + \frac{\psi_1 - \psi_2}{b}x$ where b is the panel length, x is the local abscissa and ψ_1 , ψ_2 , are the local orientation at $x=0$ and $x=b$ respectively. The stiffeners path is therefore: $dx/dy = \tan(\psi)$. We let the orientation vary between -45° and $+45^\circ$. Once the geometry of one stiffener is defined, the stiffened panel is obtained translating the stiffeners along the y -direction. It is worth nothing that, if the stiffeners are curvilinear this implies that the stiffeners spacing, measured orthogonally to the stiffeners' curve changes.

The homogenized properties are obtained equating the strain energy density between the stiffened plate and a basic repetitive cell. The criterion to select the basic repetitive cell is such that, simple translations of the cell over the plate mid-plane and along the y -axis, without overlapping, will generate the stiffened structure. Each cell contains one beam member. In order to follow the stiffener's path, the basic repetitive cell is defined as the union of sub-cells. Each sub-cell has two sides parallel to the average local orientation of the stiffeners while, the other two sides are parallel to the y -axis (Figure 2). The basic sub-cell is small enough such that the strain-energy density within the sub-cell can be approximated by a constant value. Within the sub-cell, the local orientation we considered is the average value of the stiffener orientation, that is $\psi_m = \frac{\psi_1 + \psi_2}{2}$. It follows that, within the sub-cell we neglected the effect of the curvature of the beam. This hypothesis holds if the dimensions of the sub-cell are negligible with respect to the curvature of the stiffeners.

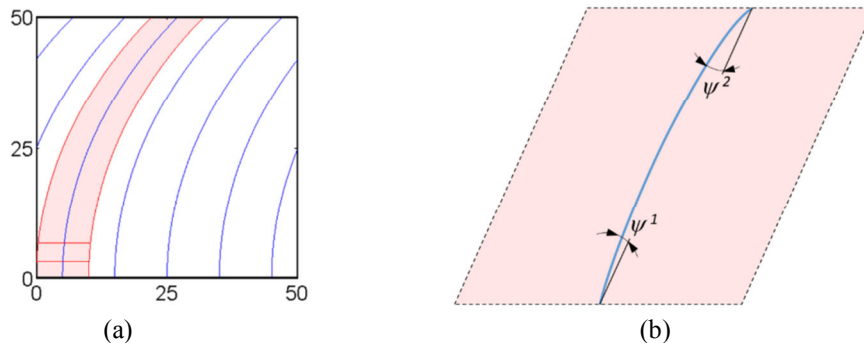


Fig. 2 - Example of basic repetitive cell (a) and detail of the sub-cell (b) for the curvilinear stiffened panel

The direct compatibility leads to the expression of the pointwise reduced stiffness matrix of the equivalent layer, reported in the equations (3) noting that, in this case, ψ varies along the x direction. The averaged strain-energy density \hat{U} (energy per sub-cell area) is defined as follows:

$$\hat{U} = \frac{1}{2} \sum_{i=1}^n \left(\frac{\sum_{j=1}^{sc} d_j \int_{L_j} \boldsymbol{\varepsilon}^T \mathbf{C} \boldsymbol{\varepsilon} dL_j}{\sum_{j=1}^{sc} A_j} \right) = \frac{1}{2} \int_0^{h_s} \boldsymbol{\varepsilon}^T \mathbf{Q} \boldsymbol{\varepsilon} dz \quad (5a)$$

$$d_j = \frac{a}{n} \cos \psi(x_j) \quad (5b)$$

where C is the beam's constitutive matrix, n is the number of stiffeners, sc is the number of sub-cells, $\boldsymbol{\varepsilon}$ is the vector of the beam's strain components expressed in terms of the plate strain components (in the global reference system $\langle xyz \rangle$), A_j is the area of the sub-cell, L_j is the sub-cell length, $d_j = a/n \cos \psi(x_j)$. On the right end of equation (3), \mathbf{Q} is the equivalent layer reduced stiffness matrix, function of the apparent engineering constants, h_s is the equivalent layer thickness, a and b are the length and width of the panel.

A parametric study has been performed to evaluate the convergence of the stiffness coefficients with respect of the number/dimension of the sub-cell. Particularly, we focused on the variation of the bending stiffness coefficients D_{ij} . In Figure 3, are reported the normalized bending coefficient ($d_{ij} = D_{ij}/\bar{D}_{ij}$) with respect to the number of sub-cell, where \bar{D}_{ij} is the asymptotic value of the corresponding coefficient. It must be clear that the bending coefficients reported are referred only to the equivalent stiffener layer. In Figure 3 (a) we show the convergence for a family of curvilinear stiffener with $\psi_1=45^\circ$ and $\psi_2=-45^\circ$ while, in Figure 3 (b) we considered $\psi_1=0^\circ$ and $\psi_2=45^\circ$. It is worth nothing that, in the first case, the convergence to the asymptotic value of the bending coefficients is slower, i.e. the number of sub-cells necessary to approach the asymptotic value is higher. This is a direct consequence of the stiffener's curvature; i.e. the higher the curvature the higher the number of sub-cells required to approximate correctly the bending stiffness. This result applies also on the membrane stiffness and the coupling matrix.

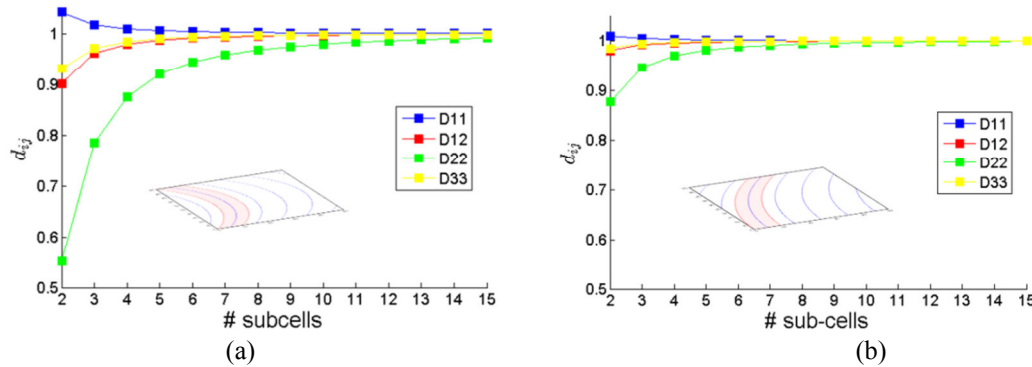


Fig. 3 - Effect of the number of the number of sub-cells on the normalized bending coefficient d_{ij} respectively for: (a) stiffened panel with $\psi_1=45^\circ$ $\psi_2=-45^\circ$ and (b) stiffened panel with $\psi_1=0^\circ$, $\psi_2=45^\circ$. The bending coefficients D_{ij} are normalized with their respective asymptotic value \bar{D}_{ij} obtained with 100-sub-cells

In Figure 4, we report the pointwise (solid line) and homogenized (dashed line) coefficients of the reduced stiffness matrix Q_{ij} , for the panel with $\psi_1=45^\circ$ and $\psi_2=-45^\circ$. The curves reported in Figure 4 are normalized with respect to the maximum of the Q_{11} coefficient. It should be noted that, since $\psi_2=-\psi_1$, the homogenized properties are such that Q_{16} and Q_{26} are both zero. That is, the resulting layer is an equivalent orthotropic layer while, in the most general case where $\psi_2 \neq -\psi_1$, the resulting layer is a 2D anisotropic layer. The expression of the stiffnesses of the equivalent layer are those reported in the equations (3).

To the authors' knowledge, none of the previous works presented in literature have extended the derivation to identify the apparent engineering constants of the equivalent stiffener layer.

During the early stages of design, reduced order models, such as beam and plate, are usually preferred to cumbersome FE computation. These models allow a first cut among all the possible solutions and can faithfully represent the behavior of the structure in terms of global responses (deformation, natural frequencies, etc.). Being understood that commercial FE codes allow introducing the values of the reduced stiffness matrix, it could be useful to extend the derivation and identify the equivalent stiffener material, thus the apparent engineering constants, that can be used directly in the analysis. It must be noted that, for straight stiffeners the stiffness (hence flexibility) matrix is singular, particularly it has rank 2. It follows that, for the straight stiffeners, is not possible to further extend the derivation for the equivalent stiffeners layer. Despite the stiffness matrix, in the local reference, is still singular, it can be proven, invoking the rank subadditivity properties, that the stiffness matrix of the equivalent stiffener layer has rank maximum if the stiffener is curvilinear. The rank subadditivity properties states, in fact, that:

$$\text{rank} \left(\sum q_i \right) \leq \sum_i \text{rank}(q_i)$$

Furthermore, by definition, $\text{rank}(q_i) = \min(m, n)$, that is:

$$\text{rank} \left(\sum q_i \right) \leq \sum_i \text{rank}(q_i) \leq \min(m, n) = \text{rank max} = m$$

We aim to prove that, if the stiffeners are curvilinear, the rank of the matrix is maximum, i.e. $\text{rank}(Q) = m$.

Proof (by contraposition)

Let us suppose that exists an angle of orientation ψ_2 , with $\psi_2, \psi_1 \in R$, $\psi_2 \neq \psi_1$ such that $\dim(Q) = \dim(q_1 + q_2)$ is not maximum, i.e. $\det(Q) = 0$.

Recalling that:

$$q_i = r_{\psi_i}^t \tilde{q} r_{\psi_i}$$

where r is the rotation of the stiffness tensor \tilde{q}^2 . The rotation is an affine transformation, i.e. the rank is preserved. Now considering the transformation given above and performing the summation, we can obtain the matrix Q . By imposing that $\det(Q) = 0$, the only real solution that exists, with multiplicity of two, is

$$\sin \psi_1 = \frac{\sin \psi_2 \cos \psi_1}{\cos \psi_2}$$

That can be written as $\tan \psi_2 = \tan \psi_1$, that is $\psi_2 = \psi_1$ which neglect our initial hypothesis.

Considering that the rank is maximum, is it possible to invert the stiffness (compliance) matrix and evaluate the apparent engineering constants of the equivalent stiffener layer.

We performed a parametric analysis to investigate the effect of the stiffeners' orientations onto the apparent engineering constants namely: extensional moduli (E_x, E_y), shear moduli

² The general form of the stiffness matrix for the stiffener is:

$$\tilde{q} = \begin{bmatrix} a & 0 & 0 \\ 0 & 0 & 0 \\ 0 & 0 & b \end{bmatrix}$$

(G_{xy} , G_{xz} , G_{yz}), Poisson's ratio (ν_{xy} , ν_{yx}), coefficients of mutual influence of the first and second kind, also known as shear-extension coupling coefficients ($\eta_{xy,x}$, $\eta_{xy,y}$) and Chentsov's coefficients (μ). Since the plate is in the concentric (thus symmetric) configuration, it is also possible to derive the apparent engineering constants of the whole laminate; i.e. skin and stiffeners. In this latter case, it is possible to extend the comparison to straight stiffeners. In Figure 5, we report the apparent engineering constants with respect to the angles ψ_1 ($x=0$), ψ_2 ($x=b$).

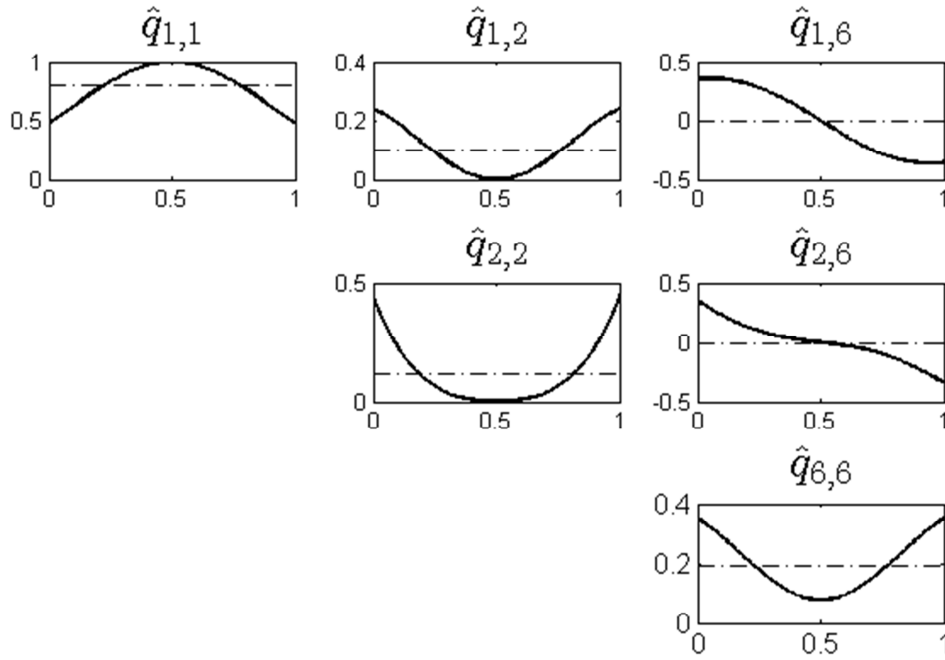


Fig. 4 - Normalized stiffness coefficients $\hat{q}_{ij} = q_{ij}/\max(q_{11})$ with respect to the non-dimensional abscissa $\hat{x} = x/b$ for a rectangular plate with $\psi_1=45^\circ$, $\psi_2=-45^\circ$. The solid line is the pointwise stiffness value while the dashed line represents the homogenized value. It is worth noting the maximum value of the q_{11} corresponds to the minimum value of the stiffener's orientation.

From Figure 5 follows that the maximum longitudinal modulus can be achieved if the stiffener are straight and aligned with the x-axis. At this configuration corresponds the maximum of the modulus G_{xz} while, the other apparent engineering constants are minimum (E_y , G_{xy} , G_{yz} , ν_{xy} , ν_{yx}) or zero. The maximum shear-extension coupling can be obtained for straight stiffeners with orientation $\psi=-35^\circ$ and $\psi=-45^\circ$ respectively for the first and second kind coefficients. The maximum shear-shear coupling is given for straight stiffeners with $\psi=45^\circ$. The maximum of the Poisson's ratio ν_{21} is at $\psi=25^\circ$, also in this case $\psi_2 = \psi_1$.

FINITE ELEMENT VALIDATION

In order to validate the procedures outlined in the previous section, we performed the buckling load analysis of a simply supported square panel (50x50 mm). The assessment is performed using two benchmark problems defined in this work. We considered first, the stiffened panel made with a family of straight stiffeners oriented at 45° , Figure 6(a); the second reference model is a stiffened panel made with curvilinear stiffeners with the following orientation: $\psi_1=45^\circ$ $\psi_2=-45^\circ$, Figure 6(b).

Both the stiffeners and plate, are made by Aluminum ($E=58000$, $\nu=0.33$). The panel thickness is 2 mm. With reference to Fig. 1 (b), the stiffeners have a rectangular cross section with $b_s=3\text{mm}$ and $h_s=1\text{mm}$. It should be noted that we are consistent with the thin-wall hypothesis, that is $h_t/b \approx 12$, where $h_t=4\text{mm}$ is the total thickness of the stiffened plate. Nonetheless, in the following, we considered also the effect of the transverse shear.

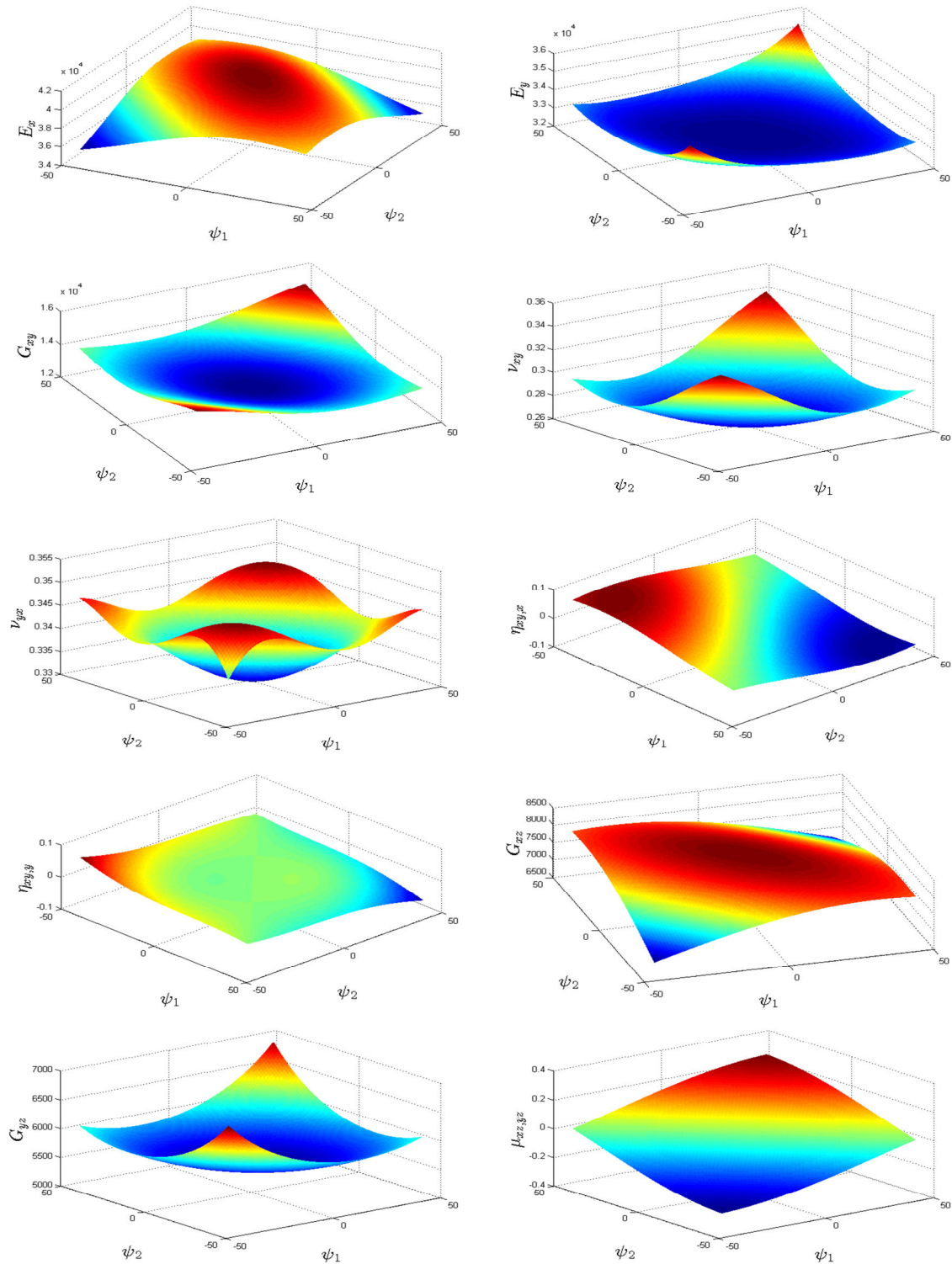


Fig. 5 - Apparent engineering constants as a function of the stiffeners orientation

The benchmark models, henceforth referred as "FE-Shell" are the reference solutions, respectively for the straight, Figure 6 (a), and curvilinear stiffeners, Figure 6 (b). The panels are subjected to uniaxial compressive load, N_x . The analysis has been performed using MSC Patran/Nastran. A small difference, in the resulting buckling load, can be noted in Table 1 if the load is distributed only on the edges of the skin panel (mode a) or also onto the stiffeners (mode b). The latter case is closer to the equivalent model that we want to validate. That is because the edge load is applied to the plate middle-surface. It should be noted that, for the straight stiffeners, the difference in the resulting buckling load is higher. That is because, when the stiffeners' orientation is such that $\psi_2 \neq -\psi_1$, we have also a bending-torsion coupling. In Figure 7 are reported the first critical load values and mode shapes for the two panels considered as benchmark.

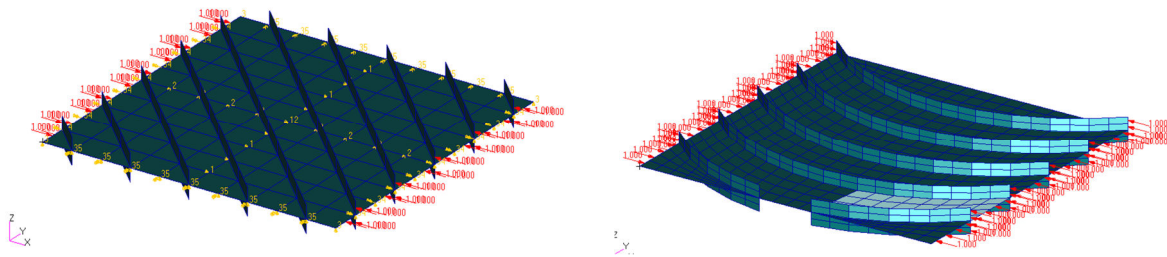


Fig. 6 - FE-Shell model adopted for the present analysis: (a) straight stiffeners oriented at $\psi=45^\circ$ and (b) curvilinear stiffeners configuration with $\psi_1=45^\circ$ and $\psi_2=-45^\circ$

Table 1 - Buckling load for the benchmark problems with mode (a) and mode (b)

Model	Buckling load, (mode a) [N/mm]	Buckling load, (mode b) [N/mm]
Straight	1299	1306
Curved	1242	1241

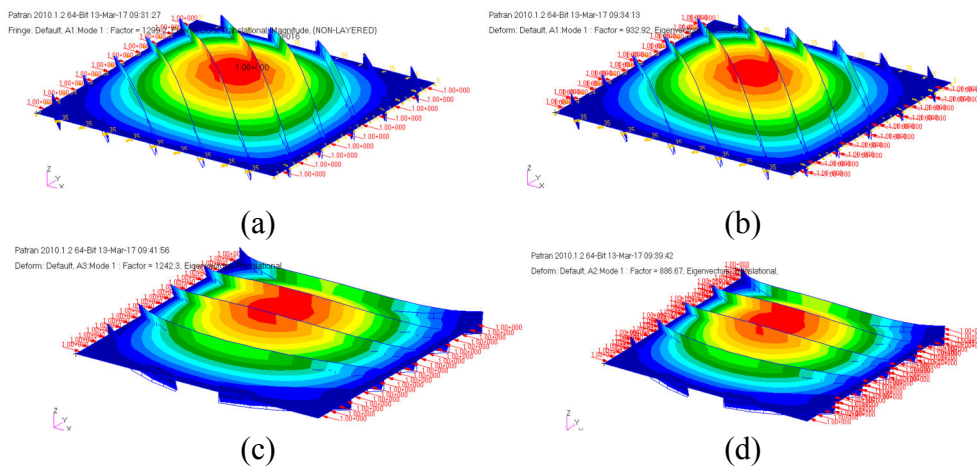


Fig. 7 - First buckling mode for the straight stiffeners oriented at 45° (a,b), and (c,d) the curvilinear stiffeners $\psi_1=45^\circ$ and $\psi_2=-45^\circ$. Load applied only to the skin (a) and (c), load applied to the skin and stiffeners (b) and (d)

The first equivalent model analyzed is the “EL-UD”, which stand for Equivalent Layer Uni-Directional. The resulting plate has three layers as shown in Figure 1(c). The apparent engineering constants can be evaluated using the equations in (4). The buckling load and the corresponding error with respect to the FEM-Shell model are reported in Table 2. The comparison is made with respect to both cases, i.e. load applied to the central skin (mode a) and to the whole stiffened panel. The error in both cases is less than 1%. Particularly, if the load is applied also the stiffeners, the discrepancy between the equivalent and the FE-Shell model is lower as we were expecting; that is because, for the equivalent model, the edge load is applied to the plate middle-surface.

Table 2 - Buckling load of the equivalent model and relative percentage error for the cases with load applied also to the stiffeners (or only to the skin of the stiffened panel)

Model	Buckling load [N/mm]	Err _R %
EL-UD	1310	0,3 (0,8)

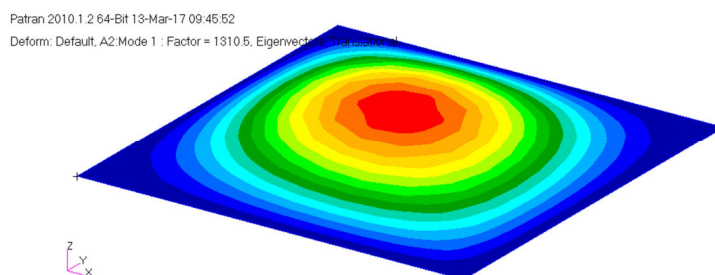


Fig. 8 - First buckling mode for the straight stiffeners oriented at 45°, EL-UD model

For the curvilinear stiffeners one might use two different approaches; (1) consider the properties of the equivalent unidirectional layer as in Cestino, 2014 and then rotate them according to the local orientation of the stiffener; (2) consider the homogenized properties. The approach described in (1) is the same used for the straight stiffeners, hence the EL-UD while, the approach in (2) is the 2D-AN-EM which stands for 2D Anisotropic Equivalent Material.

The EL-UD is a piecewise equivalent-layer model of the stiffeners for the family of curvilinear stiffeners. Along the x direction, we defined different properties for the equivalent-stiffeners layer according to the local orientation of the stiffeners. Particularly, we defined 5 and 10 properties. It is important notice that along the x direction the properties change because the stiffeners' orientation changes. The apparent engineering constants can be evaluated using the equations in (4) and taking into account that the stiffeners spacing, measured orthogonally to the stiffeners' curve, varies along the x-direction if the stiffeners are curvilinear. That is because the stiffened panel is obtained by translating the stiffener along the y-axis. It is worth noting that, the lengthwise properties are useful for the curvilinear stiffeners while useless for the straight stiffeners since, in this latter case, the properties are constant along the x direction. The different UD material properties, as well as the orientation angles are reported in Tables 3. For the sake of brevity we report, in Table 3 only the properties for the case with 5 subdivisions.

Table 3 - UD's properties for 5 subdivisions

Cell center position [mm]	5	15	25	35	45
ϑ_s [deg]	36	18	0	-18	-36
d_s [mm]	8,09	9,51	10	9,51	8,09
E_{11} [MPa]	21507,58	18295,44	17400	18295,44	21507,58
E_{22} [MPa]	0	0	0	0	0
G_{12} [MPa]	1684,49	1432,91	1362,78	1432,91	1684,49
G_{13} [MPa]	8676,25	7380,46	7019,23	7380,46	8676,25
G_{23} [MPa]	0	0	0	0	0
ν_{12}	0	0	0	0	0

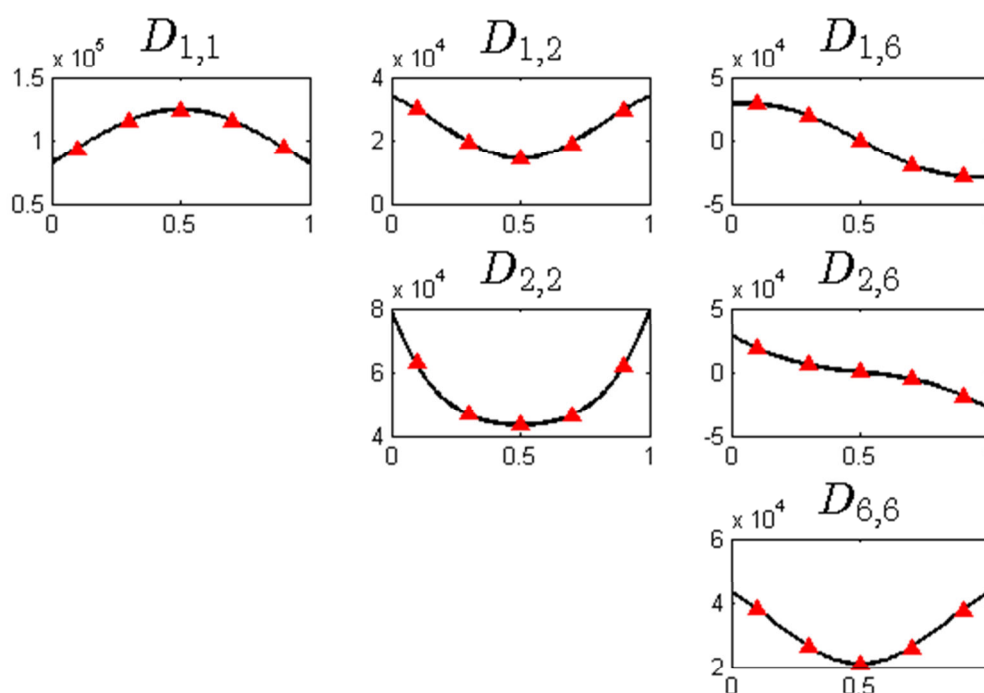


Fig. 9 - Pointwise (solid line) and local value (red markers) of the bending stiffness coefficient D_{ij} for the curvilinear stiffened panel ($\psi_1=45^\circ$ and $\psi_2=-45^\circ$). The markers are referred to the total bending coefficient obtained with the UD material listed in Table 3.

The second model considered is the homogenized model, namely "2D-AN-EM". In this case, the properties are homogenized following the procedure described in the previous section. It is worth nothing that, the homogenized properties of the equivalent-stiffeners layer can be obtained only if the stiffeners are curvilinear, as demonstrated in the previous section, unless one consider the whole laminate that is because of the rank of the matrix that has to be maximum. The mechanical properties of the resulting homogenized material, obtained using 100 sub-cells, are reported in Table 4. It should be noted that, since the orientation are $\psi_1=45^\circ$, $\psi_2=-45^\circ$ the coefficients of mutual influence and the Chentsov's coefficients are both zero. The buckling loads for the different models discussed above are reported in Table 4. The comparison is made with respect to the "FE-Shell" model with the load distributed also to the stiffeners (mode b). It should be noted as, with the increasing in the number of sub-cells the buckling load of the equivalent model converges to those of the reference model.

Table 4 - Homogenized apparent engineering constants of the equivalent stiffeners layer, for curvilinear stiffeners with $\psi_1=45^\circ$, $\psi_2=-45^\circ$.

E_x [MPa]	12318
E_y [MPa]	1833
ν_{xy}	0.602
G_{xy} [MPa]	3322
G_{xz} [MPa]	4907
G_{yz} [MPa]	1209

Table 5 - First Buckling load and percent relative error for the different models, curvilinear stiffener with $\psi_1=45^\circ$, $\psi_2=-45^\circ$.

Model	Buckling load [N/mm]	Err _R %
EL-UD (5 prop.)	1284	3,03
EL-UD (10 prop.)	1210	2,05
2D-AN-EM	1253	0,08

LIMITATIONS

This work presents the following potential source of error/limitations: (a) aeronautic panels are usually in the eccentric configuration rather than the concentric configuration considered herein; (b) typically, the stiffener's height to the plate's width ratio is $\approx 1/20$ thus, higher than those considered in this work; (c) the effect of the twisting stiffness given by the presence of the stiffener has to be considered.

CONCLUSIONS

Two equivalent models for the analysis of stiffened panels have been presented in this work. Both, straight and curvilinear stiffeners, in the concentric configuration, have been considered.

The derivation follows the procedure given in Nemeth, 2011. A homogenized method, based on the strain-energy density equivalence among the real and the equivalent structure has been used to derive the equation of the stiffnesses of the equivalent layer.

A parametric study has been performed to highlight the effect of the sub-cells dimension onto the equivalent stiffnesses. It has been shown that, the higher the curvature the higher the number of sub-cells required approaching the asymptotic value of the stiffnesses.

The formulation has been extended up to the derivation of the apparent engineering constants. It has been proven analytically that, for a single family of stiffeners, the equivalent material can be derived only if the stiffeners are in the curvilinear configuration. Contrary, the apparent engineering constants can be derived also for the straight stiffeners if one consider the whole laminate. A parametric study has been performed to show the effect of the stiffeners' geometry onto the apparent engineering constants. The parametric study aims to shed a light onto the possible couplings that may arise with the proper selection of the stiffeners geometry.

Finally, two benchmark problems have been considered to assess the validity of the procedure proposed in evaluating the equivalent stiffnesses. The comparison has been made considering the buckling loads of a simply supported stiffened square panel. In both cases, one family of stiffeners has been considered. A good agreement between the complete model (skin plate and stiffeners) and the equivalent model have been obtained for both the configurations considered namely, straight and curvilinear stiffeners.

REFERENCES

- [1]-Benscoter, S. U.; and MacNeal, R. H.: Equivalent Plate Theory for a Straight Multicell Wing. NACA TN 2786, 1952
- [2]-Cestino E. Frulla G.; (2014). Analysis of slender thin-walled anisotropic box-beams including local stiffness and coupling effects. AIRCRAFT ENGINEERING AND AEROSPACE TECHNOLOGY, vol. 86 n. 4, pp. 345-355
- [3]-Chen, H.-J.; and Tsai, S. W.: Analysis and Optimum Design of Composite Grid Structures. Journal of Composite Materials, vol. 30, no. 4, 1996, pp. 503-534
- [4]-Crawford, R. F.; and Libove, C.: Shearing Effectiveness of Integral Stiffening. NACA TN 3443, 1955
- [5]-Dow, N. F.; Libove, C.; and Hubka, R. E.: Formulas for the Elastic Constants of Plates with Integral Waffle-Like Stiffening. NACA Rep. 1195, 1953
- [6]-Flugge, W.: Die Stabilität der Kreiszyinderschale. Ingenieur-Archiv, vol. 3, no. 5, 1932, pp. 463-506
- [7]-Gomza, A.; and Seide, P.: Minimum-Weight Design of Simply Supported Transversely Stiffened Plates under Compression. NACA TN 1710, 1948
- [8]-Gürdal Z., Tatting B. F., Wu C.K., Variable stiffness composite panels: Effects of stiffness variation on the in-plane and buckling response, Composites: Part A 39 (2008) 911-922
- [9]-Heki, K.; and Saka, T.: Stress Analysis of Lattice Plates as Anisotropic Continuum Plates. IASS Pacific Symposium - Part II on Tension Structures and Space Frames, Tokyo and Kyoto, October 17-23, 1971, pp. 7-7-1 to 7-7-12
- [10]-Hoppmann, W. H., II and Magness, L. S.: Nodal Patterns of the Free Flexural Vibrations of Stiffened Plates. Journal of Applied Mechanics, December, 1957, pp. 526-530
- [11]-Hoppmann, W. H., II: Bending of Orthogonally Stiffened Plates. Journal of Applied Mechanics, June, 1955, pp. 267-271
- [12]-Hoppmann, W. H., II: Elastic Compliances of Orthogonally Stiffened Plates. Proceedings of the Society of Experimental Stress Analysis, vol. 14, no. 1, 1956, pp. 137-144
- [13]-Hoppmann, W. H., II; Huffington, N. J., Jr.; and Magness, L. S.: A Study of Orthogonally Stiffened Plates. Journal of Applied Mechanics, September, 1956, pp. 343-350
- [14]-Huber, M. T.: Die Grundlagen einer rationellen Berechnung der Kruezwise beweheten Eisenbetonplatten. Zeitschrift des Oesterreichischen Ingenieur und Architekten-Vereines, vol. 66, 1914, pp. 557-564

- [15]-Huber, M. T.: Die Theorie der Kreuzweise bewehrten Eisenbeton-Platte nebst Anwendungen auf mehrere bautechnisch wichtige Aufgaben uiber rechteckige Platten. Bauingenieur, vol. 4, 1923, pp. 354-360 and 392-395
- [16]-Huber, M. T.: Probleme der Statik Technisch Wichtiger Orthotroper Platten. Nakkadem Akadenji Nauk Technicznych Warszawa, Poland, 1929
- [17]-Huffington, N. J., Jr.: Theoretical Determination of Rigidity Properties of Orthogonally Stiffened Plates. Journal of Applied Mechanics, March, 1956, pp. 15-20
- [18]-Jaunky, N.; Knight, N. F., Jr.; and Ambur, D. R.: Formulation of an Improved Smeared Stiffener Theory for Buckling Analysis of Grid-Stiffened Composite Panels. NASA TM 110162, 1995. 117
- [19]-Jaunky, N.; Knight, N. F., Jr.; and Ambur, D. R.: Formulation of an Improved Smeared Stiffener Theory for Buckling Analysis of Grid-Stiffened Composite Panels. Composites: Part B, vol. 27B, 1996, pp. 519-526
- [20]-Kapania R. K., Li J., Kapoor H., Optimal Design of Unitized Panels with Curvilinear Stiffeners, AIAA 5th Aviation, Technology, Integration, and Operations Conference (ATIO)/ 26 - 28 Sep 2005, Hyatt Regency Crystal City, Arlington, Virginia
- [21]-Kennedy G. J.; Kenway G. K. W.; and Martins J. R. R. A, High Aspect Ratio Wing Design: Optimal Aerostructural Tradeoffs for the Next Generation of Materials, Proceedings of the AIAA Science and Technology Forum and Exposition (SciTech), 2014
- [22]-Mulani S. B., Locatelli D., Kapania R. K., Grid-Stiffened Panel Optimization using Curvilinear Stiffeners, 52nd AIAA/ASME/ASCE/AHS/ASC Structures, Structural Dynamics and Materials Conference 19th 4 - 7 April 2011, Denver, Colorado
- [23]-Mulani, S. B., Joshi P., Li P., Kapania R. K., and Shin Y. S., Optimal Design of Unitized Structures Using Response Surface Approaches, JOURNAL OF AIRCRAFT, Vol. 47, No. 6, November-December 2010
- [24]-Nemeth M. P., A Treatise on Equivalent-Plate Stiffnesses for Stiffened Laminated-Composite Plates and Plate-Like Lattices. Tech. rep. NASA/TP-2011-216882. NASA, Langley Research Center, Jan. 2011
- [25]-Pfluger, A.: Zum Beulproblem der anisotropen Rechteckplatte. Ingenieur-Archiv, vol. 16, 1947, pp. 111-120
- [26]-Pshenichnov, G. I.: A Theory of Latticed Plates and Shells. Series on Advances in Mathematics for Applied Sciences-vol. 5, World Scientific, New Jersey, 1993
- [27]-Slinchenko, D.; and Verijenko, V. E.: Structural analysis of Composite Lattice Shells of Revolution on the Basis of Smearing Stiffness. Composite Structures, vol. 54, 2001, pp. 341-348
- [28]-Smith, C. B.; Heebink, T. B.; and Norris, C. B.: The Effective Stiffness of a Stiffener Attached to a Flat Plywood Plate. Report No. 1557, U. S. Department of Agriculture, Forest Products Laboratory, September, 1946
- [29]-Tamijani A. Y. and Kapania R. K. Buckling and Static Analysis of Curvilinearly Stiffened Plates Using Meshfree Method, 50th AIAA/ASME/ASCE/AHS/ASC Structures, Structural Dynamics, and Materials Conference 17th 4 - 7 May 2009, Palm Springs, California
- [30]-Wang D. and Abdalla M. M., Global and local buckling analysis of grid-stiffened composite panels, Composite Structures, Vol 119, pages 767 - 776, 2015

[31]-Wang D., Abdalla M. M., Buckling optimization of steering stiffeners for grid-stiffened composite structures, 20th International Conference on Composite Materials Copenhagen, 19-24th July 2015

[32]-Won, C. J.: Stiffened Plates with Arbitrary Oblique Stiffeners. International Journal of Solids and Structures, vol. 26, 1990, pp. 779-799

[33]-Wu C. K., Gürdal Z., and J. H. Starnes, Structural response of compression loaded, tow-placed, variable stiffness panels, Proceedings of the 43rd AIAA/ASME/ASCE/AHS/ASC structures, structural dynamics and materials conference, Denver, Co, 2002, pp. 2002-1512

APPENDIX A

APPARENT ENGINEERING CONSTANTS

The engineering constants are behavioural constants with obvious physical interpretation. For this reason, it is a common practice derive these values instead of dealing with the compliance or stiffness matrices. The derivation can be performed regardless starting from the stiffness or from the compliance matrix even though, the derivation from the compliance, is more immediate. Provided the matrices have full rank, the engineering constant are given as follows:

$$E_1 = \frac{1}{S_{11}} = \frac{\Delta}{Q_{26}^2 - Q_{22}Q_{66}} = E_x$$

$$E_2 = \frac{1}{S_{22}} = \frac{\Delta}{Q_{16}^2 - Q_{11}Q_{66}} = E_y$$

$$G_{12} = \frac{1}{S_{66}} = \frac{\Delta}{Q_{12}^2 - Q_{11}Q_{22}} = G_{xy}$$

$$\nu_{12} = -E_1 S_{21} = -\frac{Q_{12}Q_{66} - Q_{16}Q_{26}}{Q_{26}^2 - Q_{22}Q_{66}} = \nu_{xy}$$

$$\nu_{21} = -E_2 S_{12} = -\frac{Q_{12}Q_{66} - Q_{16}Q_{26}}{Q_{16}^2 - Q_{11}Q_{66}} = \nu_{yx}$$

$$\eta_{12,1} = -G_{12} S_{16} = \frac{Q_{22}Q_{26} - Q_{12}Q_{26}}{Q_{12}^2 - Q_{11}Q_{22}} = \eta_{xy,x}$$

$$\eta_{12,2} = -G_{12} S_{26} = \frac{Q_{11}Q_{26} - Q_{12}Q_{26}}{Q_{12}^2 - Q_{11}Q_{22}} = \eta_{yx,y}$$

where $\Delta = -(Q_{66}Q_{12}^2 - 2Q_{12}Q_{16}Q_{26} + Q_{22}Q_{16}^2 + Q_{11}Q_{26}^2 - Q_{11}Q_{22}Q_{66})$

$$G_{23} = \frac{1}{S_{44}} = \frac{\Delta_T}{Q_{T22}} = G_{yz}$$

$$G_{13} = \frac{1}{S_{55}} = \frac{\Delta_T}{Q_{T11}} = G_{xz}$$

$$\mu_{13,23} = -G_{13} S_{45} = \frac{Q_{T12}}{Q_{T11}} = \mu_{xz,yz}$$

where $\Delta_T = Q_{T11}Q_{T22} - Q_{T12}^2$